Automated Polyaxial Screw Placement Using a Commercial-Robot-Based, Image-Guided Spine Surgery System

Alexander D. Smith, Jacob Chapin, Paul V. Birinyi, Prathamesh V. Bhagvath, and Andrew F. Hall, *Member, IEEE*

***Abstract*—Robotic spine surgery systems, used for placing pedicle screws, have been in clinical use since 2004; however, these systems act only as a positioner for guide tubes, which the surgeon uses to manually advance tools to prepare the site and place hardware (e.g., pedicle screws). This article presents the development, operation, and evaluation of a new, commercial-robot-based, image-guided surgery system that automates the process of bone preparation and polyaxial screw placement. The system is based on the KUKA LBR iiwa 7-axis collaborative robot. Fiducial marker and screw locations are defined on a pre-operative CT image using the 3D Slicer open source image visualization platform. The system uses the robot's internal localization system for registration, by touching fiducial markers in a hand-guiding mode. A rotary-motor end effector with exchangeable tools is used for both hole-drilling and screw placement. A novel single-motor based mechanism was developed for placing polyaxial pedicle screws. An accuracy test was performed by placing polyaxial screws in synthetic vertebrae which mimic the mechanical properties of human bone. In placing 10 screws, the entry point accuracy was 0.49 ± 0.17 mm and the destination point accuracy was 1.49 ± 0.46 mm. The results compare favorably to evaluations of commercial robotic spine surgery systems.**

***Index Terms*—Image guided surgery, medical robotics, pedicle screw placement, robotic spine surgery.**

Manuscript received June 25, 2020; revised September 3, 2020 and October 15, 2020; accepted November 3, 2020. Date of publication November 11, 2020; date of current version February 22, 2021. This article was recommended for publication by Associate Editor D.-S. Kwon and Editor P. Dario upon evaluation of the reviewers' comments. *(Alexander D. Smith and Jacob Chapin contributed equally to this work.) (Corresponding author: Andrew F. Hall.)*

Alexander D. Smith was with the Department of Biomedical Engineering, Parks College of Engineering, Aviation and Technology at Saint Louis University, St. Louis, MO 63103 USA. He is now with the Carle Illinois College of Medicine, Champaign, IL 61820 USA (e-mail: ads10@illinois.edu).

Jacob Chapin was with the Department of Biomedical Engineering, Parks College of Engineering, Aviation, and Technology, Saint Louis University, St. Louis, MO 63103 USA. He is now with NAZ Supply CAPEX Division, Anheuser-Busch Company, St. Louis, MO 63118 USA (e-mail: jacob.chapin@slu.edu).

Paul V. Birinyi was with the Department of Neurosurgery, Saint Louis University School of Medicine, St. Louis, MO 63104 USA. He is now with Alexandria Neurosurgical Clinic, Alexandria, LA 71301 USA (e-mail: pbirinyi@gmail.com).

Prathamesh V. Bhagvath and Andrew F. Hall are with the Department of Biomedical Engineering, Parks College of Engineering, Aviation, and Technology, Saint Louis University, St. Louis, MO 63103 USA (e-mail: prathameshvishnudas.bhagvath@slu.edu; andy.hall@slu.edu).

Digital Object Identifier 10.1109/TMRB.2020.3037339

I. Introduction

IMAGE-GUIDED, robotic spine surgery is an expanding field, with an annual composite growth rate over the next five years estimated at between 9% and 22% [1], [2], [3]. Currently, the primary application for these systems is the placement of pedicle screws during spinal fusion and fixation surgery, a treatment for degenerative spinal disease and instability [4]. In this procedure, the diseased disc between two (or more) vertebrae is first removed and replaced by a cage-like device which is often filled with bone graft material. For additional support, and to allow the fusion to occur between immobile bones, screws often are placed on both sides of each vertebra, in the pedicles. The heads of these screws, known as tulip-head screws, typically are polyaxial (able to angulate around the shaft) and also are slotted, such that a rod can be fit into the slot, connecting two or more screws on a particular side. The slotted heads are threaded on the inside, such that the rod may be locked into place with a small set screw. The cage and pedicle screws form three points of support that lock the vertebrae together. This is illustrated in Fig. 1. For many patients, this procedure eliminates or reduces the back pain caused by a degenerative and unstable spinal segment and can help radicular pain caused by compression of the spinal nerve roots. The most common example of this procedure is the transforaminal lumbar interbody fusion (TLIF) procedure [5].

Image-guided robotic spine surgery systems generally consist of a surgical planning computer, a robotic arm or similar positioning device, and a means to register the 3D image coordinate system to the operating field coordinate system (containing the robot and the patient), such that the robot can access the screw locations on the patient as defined in the images. During the procedure, the surgical planning computer first imports preoperative or intraoperative images that are used by the surgeon to plan the location (entry point and destination) of the pedicle screws. The images are then registered to the robot/patient coordinate system. The robot then positions a guiding tube (its end effector) at the locations and angles required for placement of each of the screws. At each of these locations the surgeon manually prepares the site (e.g., drills a hole) and manually places the pedicle screws using the guide positioned by the robot.

There are currently four commercial image-guided spine surgery robots. Interestingly, each has been acquired by one of the major medical device companies. The Mazor Renaissance

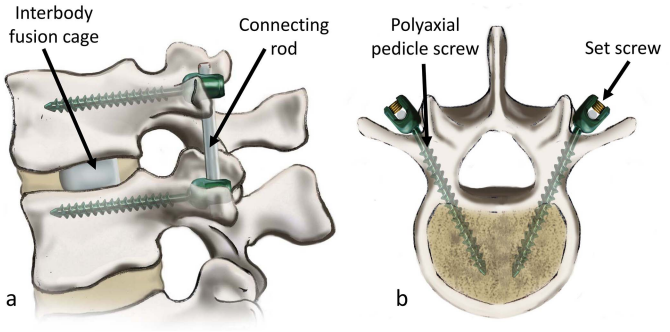

Fig. 1. Sagittal (a) and axial (b) view of lumbar vertebra with pedicle screws inserted.

TABLE I
ROBOTIC SURGERY SYSTEM CLASSIFICATIONS (ADAPTED FROM [22] AND [23])

1. Surgical CAD/CAM (Image-Guided) Robots
1.a Supervisory Controlled Autonomous Robots
1.b Shared Control Robots
2. Surgical Assistant Robots
2.a Surgeon Extender Robots
2.b Auxiliary Support Robots

(Medtronic, Dublin, Ireland) (formerly branded Spine Assist) was the first device commercialized (2004). The robot is patient (bone) mounted and is based on a 6-UPS (universal prismatic spherical) parallel mechanism [6], [7]. A preoperative CT is used for screw placement planning. Registration is accomplished via two fluoroscopic images, which capture both the spine and fiducial markers on the robot mount. Once registration is complete the system determines the location that the robot is to be positioned on the mount, to guide placement of a particular screw.

The Mazor-X (Medtronic, Dublin, Ireland) is based on a more traditional 6 degree-of-freedom (DOF) cart-mounted robotic arm. The registration mechanism is similar to the Renaissance, but an optical instrument navigation system [8] can be added so that the location of the tools inserted in the tube can be visualized on the surgical planning computer. Optical navigation systems are already widely used in spine surgery, on tools held directly by surgeons, to create a virtual image of screw insertion [9], [10].

The ROSA system (Zimmer Biomet, Warsaw, IN) also uses a cart-mounted 6 DOF robotic arm, and has an integrated optical navigation system. It supports both fluoroscopic imaging and intraoperative cone-beam CT (e.g., O-arm) imaging [11]. Registration of the anatomy to the robot is accomplished by positioning a radiographic fiducial marker grid, held by the robot, within the fluoroscopy images (two required) or O-arm image of the spine. The navigation system is registered via optical markers placed both on the patient and on the robot.

The most recent system, ExcelsiusGPS (Globus Medical, Inc., Audubon, PA) also is based on a cart-mounted 6 DOF robotic arm with an integrated optical navigation system. It can use preoperative CT, intraoperative CT or fluoroscopy for planning and end-effector positioning. In one operational example [12], a fiducial marker array is placed on the patient prior to an O-arm scan of the spine, which can be identified both in the image and by the optical navigation system. The robot is registered to the optical navigation system via active navigation markers (lights) on the robot.

Over 36,000 robotic spine procedures have been performed since 2004; the majority by the Mazor systems [13]. There have been several review articles published recently, evaluating the potential advantages of this nascent technology on screw placement accuracy, procedure time, radiation dose, safety, recovery time, and cost effectiveness [14], [15], [16], [17], [18]. Whereas placement accuracy and radiation exposure to the surgeon are generally improved when compared to free-hand techniques, there is a dearth of studies comparing robotic systems to non-robotic navigation systems. There is no clear trend yet on improvements in procedure time, recovery time, or cost effectiveness.

Prior to these commercial systems, several systems were developed by research intuitions. Examples include a system based on a predecessor of the KUKA LBR robot, developed by Ortmaier *et al.* in 2006 [19], the Biplane Fluoroscopy Guided-Robot System (BFRS) developed by Kim *et al.* in 2010 [20], and the Robotic Spinal Surgical System (RSSS) developed by Tian *et al.* in 2014 [21]. While their system details vary, they share the same basic components and operate in much the same manner as the commercial systems.

Whereas two of the research systems drill holes in the spine [19], [21], the commercial robotic systems provide only a properly positioned and aligned guiding tube, through which the spine surgeon manually prepares for and/or places the pedicle screws. It is useful to consider the operation of these systems in the context of robotic surgery system classifications and capabilities.

We combined classifications from Taylor and Stoianovici [22] and from Nathoo *et al.* [23], which resulted in the two-level classification system shown in Table I. *Auxiliary Support* robots are not directly involved in the surgical procedure but instead perform support functions such as endoscope or retractor holding and manipulation. *Surgeon Extender* robots are controlled directly, in real-time, by the surgeon and often augment the surgeon's ability. The most prominent example is the daVinci Surgical System (Intuitive Surgical, Sunnyvale, CA). *CAD/CAM* or *Image-Guided* robots include *Shared Control* robots and *Supervisory Controlled Autonomous* robots. All current commercial image-guided robotic spine surgery systems are of the *Shared Control* variety as the systems provide a properly positioned and oriented channel through which to insert tools, but the surgery itself is left to the surgeon.

It is interesting that, in spite of the extraordinary technologies integrated into commercial robotic spine surgery systems, the final steps of drilling and screw placement are left to the surgeon. This is in contrast to other industries, such as robotic welding, where the robot performs the complete task automatically.

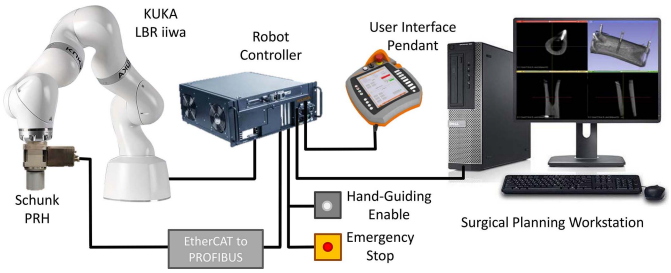

Fig. 2. KUKA LBR-based, image-guided robotic spine surgery system block diagram.

Our goal was to develop a system for spine surgery that was categorized as a *Supervisory Controlled Autonomous* robot, where the entire process of preparing bone, and inserting spine screws was automated. While a system of this type has many important specifications and features, the most important evaluation criterion is screw placement accuracy. Without clinically acceptable placement accuracy, the system is not viable. Here we describe the design and operation of this new system and the first ex-vivo accuracy study.

II. System Architecture

The system consists of four primary components: the robot, a continuous rotary unit, a set of exchangeable tools, and a surgical planning workstation. A system block diagram is shown in Fig. 2.

A. Robot

The surgery system is based on a KUKA LBR iiwa 7 R800 7-axis robotic arm (KUKA, Augsburg, Germany). Additional subsystem components include a robot controller/power supply unit with an embedded PC running Windows, and a user interface pendant. The robot has a positional repeatability of 0.1 mm, and a maximum payload of 7 kg. Robot software is developed in Java on a Windows PC, using a development environment provided by KUKA. The robot's internal localization system is used for both registration and screw placement, as there is no integrated external navigation system.

B. Rotary Unit

Continuous rotation, for drilling holes and placing screws, is provided by a Schunk PRH 060-100-PB-065 rotary unit end effector (Schunk GmbH & Co. KG, Lauffen am Neckar, Germany). The unit has a maximum revolution rate of 1 r/s, and a maximum torque of 11 Nm. The unit is controlled programmatically by the robot controller via EtherCAT and an EtherCAT-to-PROFIBUS interface module (EL 6731, Beckhoff Automation GmbH & Co. KG, Verl, Germany).

C. Tool Exchanger and Surgical Tools

The tool exchanger, tool kit, tool rack and screw rack are shown in Fig. 3 and were designed in our lab. The tools were machined from stainless steel, and the racks were 3D printed in polylactic acid (PLA).

The exchanger mechanism is permanent-magnet based (neodymium-iron-boron alloy), with oppositely polarized magnets on the tool exchanger and each of the tools. Tools are engaged by the end effector (which is attached to the rotary unit) via magnetic attraction and then slid sideways out of the tool rack (Fig. 3). A series of posts on the tool and matching holes on the tool exchanger allow the transfer of torque from the rotary unit to the tool tip. Tools include the hand-guided registration tool, a drill bit, and a screwdriver mechanism for polyaxial screws.

D. Polyaxial Screw Driver End Effector

Polyaxial screws (Figs. 4a and 4c) have a hex (or Torx®) bit receptacle in the shaft, used to drive the screw, and a threaded swiveling head. The threads in the head are used to fix the fusion rods, once the screw is placed (Fig. 1), but these threads are also used to align the swivel head to the shaft during screw placement. A manual polyaxial screw driver (Figs. 4b and 4c) contains two concentric shafts. The inner shaft has a hex bit, to engage the screw shaft, and the outer shaft has threads to engage the head.

A *manual* polyaxial screwdriver requires two-handed operation. For screw attachment, the inner shaft is slid distally through the outer shaft, and rotated, to engage the hex receptacle. The outer shaft is then slid distally and also rotated, to engage the threads in the head which align the head to the screw shaft and fix it in place (Fig. 4c). The screw is placed using the inner shaft to apply torque to the hex receptacle on the screw shaft. Once placed, the driver is removed by rotating the outer shaft to disengage the threads in the head, while keeping the hex bit fixed with the surgeon's other hand.

Our goal in screwdriver end effector design was to place commercially available polyaxial screws. We therefore sought to implement a device that requires two independent controls (both of the surgeon's hands). A straightforward approach might involve two independently controlled motors connected to concentric shafts, with the outer shaft connected via a gearing mechanism. Alternatively, the Schunk motor has a through-hole along its axis, so a second motor could be added in back of it to control the inner concentric shaft.

The design presented here obviates the requirement for a second motor by shifting the application of driving torque from the inner shaft to the outer shaft. Using this approach, the only function of the inner shaft, in addition to screw alignment, is to remain stationary during screw driver disengagement, so that the screw cannot rotate as the driver disengages.

This end effector was designed and constructed using a modified manual polyaxial screwdriver and a single Schunk rotary unit (Fig. 5). In this design the hex bit was milled into a cylinder, so that the driver tip can engage the screw's hex bit receptacle regardless of its angular orientation (i.e., can be easily engaged by the robot without the requirements to rotate the tip and sense engagement of the hex bit). The inner shaft extends through the rotary unit and into an assembly containing a one-way bearing, such that the inner shaft can rotate passively during clockwise rotation as the screw is picked up

® Registered trademark.

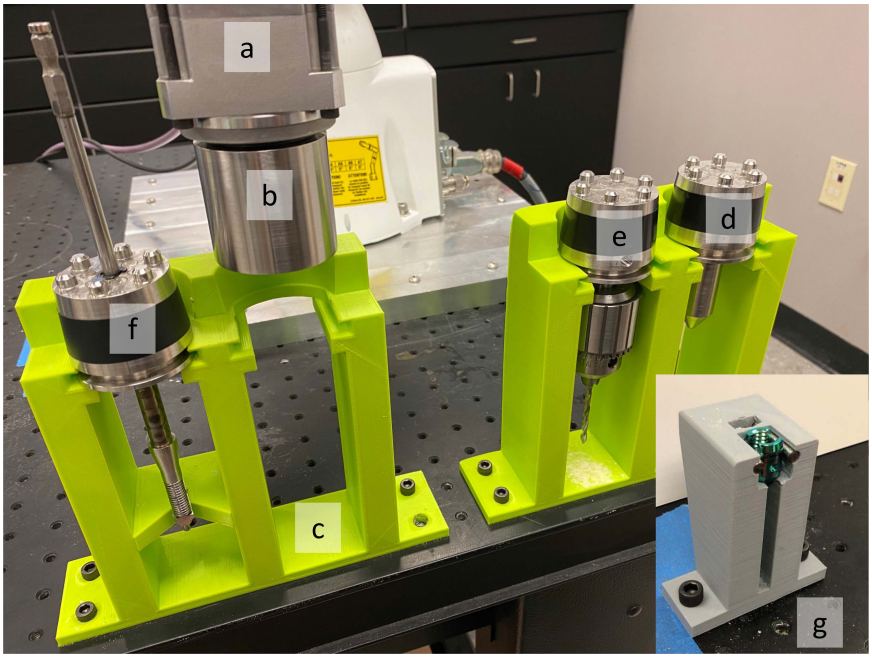

Fig. 3. Robot end effector and accessories. (a) Schunk PRH rotary unit. (b) Magnetic tool exchanger. (c) Tool rack. (d) Hand registration tool. (e) Drill bit tool. (f) Polyaxial screw driver tool. (g) Screw rack.

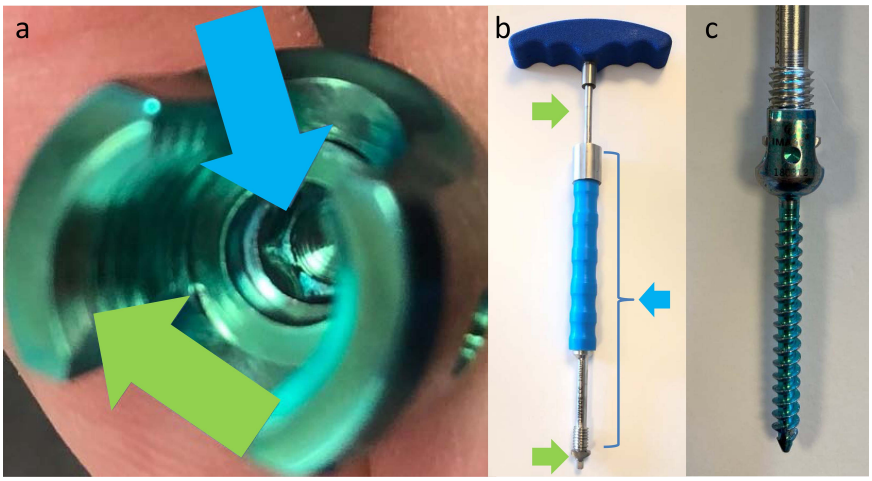

Fig. 4. (a) Polyaxial spine screw with hex receptacle on the body (blue arrow) and threaded swivel head (green arrow). (b) Manual polyaxial screw driver with inner (green arrow) and sliding outer (blue arrow) concentric shafts. (c) Screw driver with polyaxial screw affixed.

and placed, but is fixed during counterclockwise rotation as the screwdriver disengages, holding the screw in place via a pair of *wings* that engage the slots on the screw head (Fig. 5 insert). This mechanism enables the robot to pick up a screw from the screw rack, place it in the spine, and disengage the screwdriver, leaving the screw in place.

E. Surgical Planning Workstation

This subsystem is a Linux-based PC running 3D Slicer, an open-source medical image visualization platform (slicer.org). Pre-operative images can be imported for the purpose of identifying the locations of fiducial markers, and for planning screw placement. These locations are transferred to the robot controller over ethernet using the OpenIGTLink protocol [24]. This workstation is also used to measure placement accuracy.

III. System Operation

Performing automatic screw placement involves user interaction with both the surgical planning workstation and the robot. This workflow is shown in Fig. 6. A CT image of the target bone, which had fiducial markers implanted prior to scanning, is imported into 3D Slicer. Fiducial markers are identified, and screw locations planned, using the standard orthogonal image planes and a volumetric rendering. These coordinates are sent by the user to the robot upon request.

A. Tool Engagement

At the start of robot program operation, the robot picks up the fiducial marker registration tool. The robot approaches the tool from above in a compliant movement mode, while rotating the tool exchanger. This allows the posts on the tools

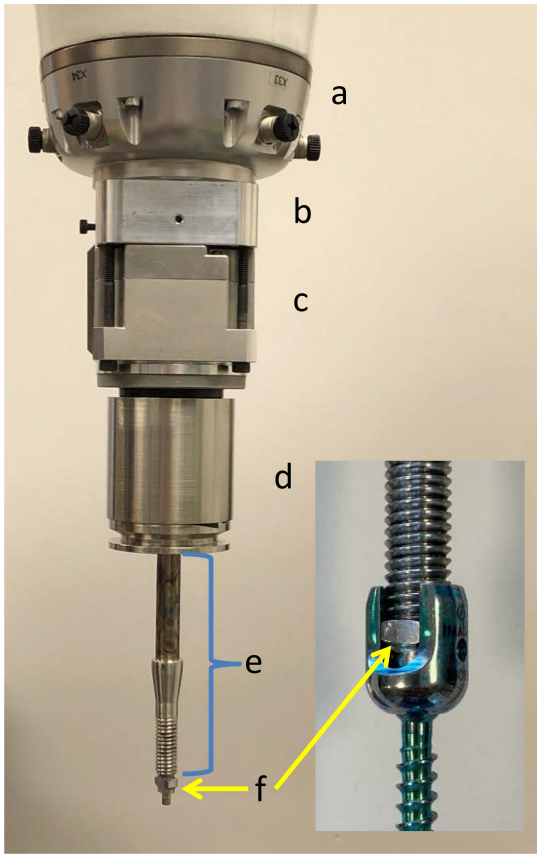

Fig. 5. Polyaxial screw driver end effector attached to KUKA LBR (a) with (b) one way bearing assembly, (c) Schunk rotary motor, (d) magnetic tool exchanger, (e) outer shaft, and (f) inner shaft. The inner shaft goes through the tool exchanger and rotary motor to engage the one way bearing. The inset image shows the wings of the inner shaft sitting in the slots of the screw head, which prevent rotation of the screw head during screwdriver disengagement.

to engage the holes in the tool exchanger, and the magnets on both to engage, holding the tool in the exchanger. The tool is then slid out of the rack horizontally. All tools are engaged in this manner.

B. Coordinate System Registration

In order to translate screw locations defined in the CT image (via 3D Slicer) to locations in the robot coordinate system, the coordinate systems must be registered. For this process the system relies on fiducial markers that have been placed on the spine which are physically sampled by the robot. The robot has a built-in hand guiding mode, common to many collaborative robots, where each of the individual axes can be manipulated by the user. In this mode, the user navigates the registration end effector to each of the implanted fiducial markers, as shown in Fig. 8. Each fiducial marker location is recorded by the robot controller which uses this data, along with the fiducial marker locations identified by the user in the pre-operative image, to register the coordinate systems. We used a closed-form registration algorithm based on matrix singular value decomposition, described by Arun *et al.* [25].

C. End Effector Positioning and Pilot Hole Creation

The screw entry and destination points are sent from the surgical planning workstation to the robot controller where they are transformed into robot coordinates. The screw insertion point, the two insertion angles (orthogonal to the end effector axis), and the screw depth are then computed. The robot then picks up the drill and moves to a location that is 50 mm away from the insertion point, along the screw axis. This is done to avoid any contact between the drill bit tip and the spinous or transverse processes during navigation. It then orients the end effector and advances 50 cm along the screw axis to the insertion point, creating a pilot hole in the bone for the screw. Due to the low rotation rate of the rotary unit (1.0 r/s), the drill was advanced at a rate of 0.1 mm/s. The drill bit was custom manufactured with a tip angle of 50°. This obviated the need for an awl, thereby reducing the number of tools required.

D. Screw Placement

After replacing the drill tool the robot picks up the screw driver, moves to the screw rack, and picks up a polyaxial screw. The screw rack holds the screw head in a specific orientation and does not allow rotation, so that the robot can advance the inner shaft into the hex receptacle while rotating the outer shaft to engage the screw head threads (Fig. 9a). This step ends when the robot distal axis torque exceeds a threshold of 0.3 Nm. During this process, the screw distal tip is engaged in a shallow hole to maintain a vertical orientation. Once engaged, the screw is lifted slightly and moved horizontally out of the rack.

The robot then moves to a location above the entry point, as described above, and orients the tool (Fig. 9b) before advancing to the entry point. The rotary unit is turned on and the screw is advanced at a rate to match the screw thread spacing over the computed insertion distance (Fig. 9c). The rotary unit then reverses direction and the screw driver is retracted as the threaded outer shaft disengages from the threads in the screw head. The one-way bearing in the screwdriver mechanism prohibits inner shaft rotation, which holds the screw in place during disengagement. The process is then repeated for subsequent screws.

IV. Screw Placement Accuracy Evaluation

Screw placement accuracy is a gating requirement for any automated spine surgery system. Accordingly, our initial focus in system evaluation was a quantitative evaluation of screw placement accuracy.

A. Methods

A total of ten 50 mm polyaxial pedicle screws (ZealMAX Innovations LTD, India) were placed in 5 synthetic, L3 or L4, lumbar vertebrae (Sawbones USA, Vashon Island, WA). These biomechanical models contain both cortical and cancellous bone components designed to mimic the mechanical properties of those in human vertebrae. Four headless screws (aka hanger bolts) were placed in each of the vertebrae as fiducial markers (Fig. 8).

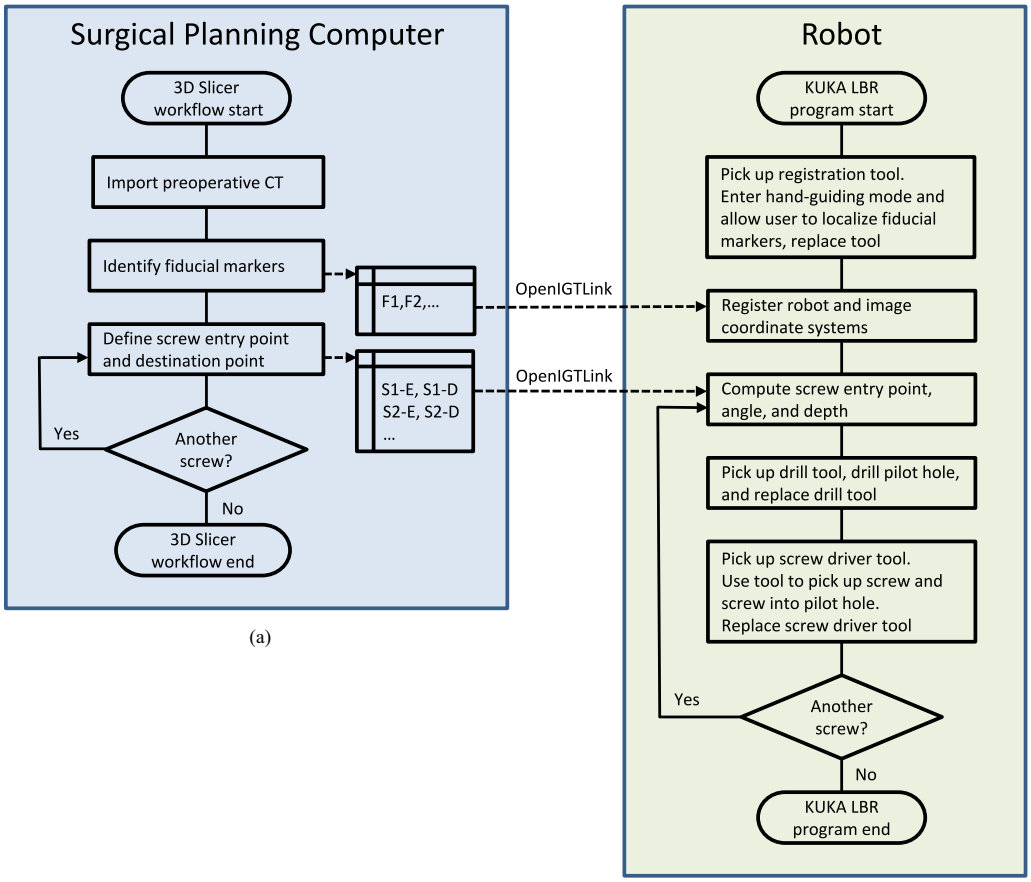

(a)

(b)

Fig. 6. Workflow block diagrams. (a) Workflow diagram for the surgical planning workstation. (b) Workflow block diagram for the robot.

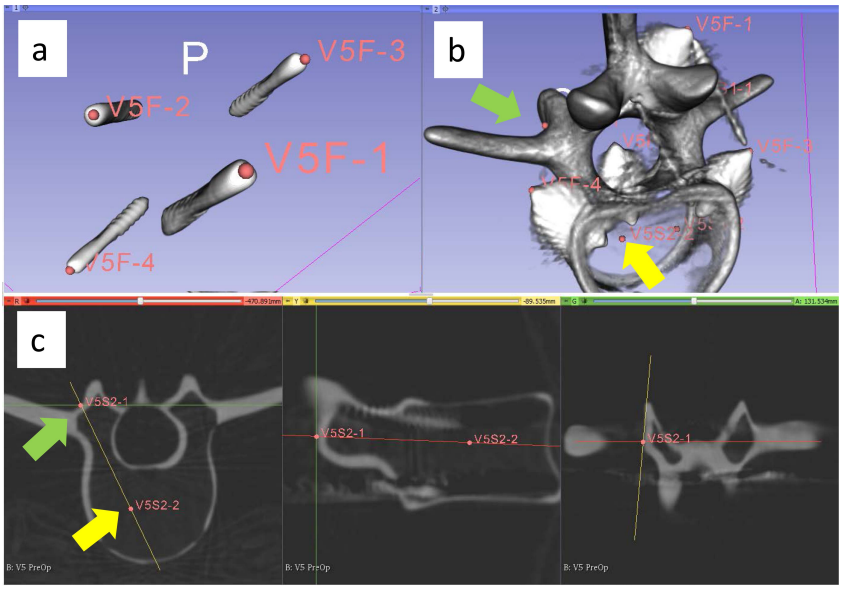

Fig. 7. Pre-operative C-arm CT image of synthetic vertebra displayed on surgical planning workstation. Reformatted planar views were used to identify both the fiducial marker tips and the screw path plan (entry and destination points). Point locations were verified using volume renderings. (a) Fiducial markers shown in a volume rendering. (b) Screw entry (green arrow) and destination (yellow arrow) points shown in a volume rendering (windowed to visualize the vertebra). (c) Reformatted multiplanar views showing a screw entry (green arrow) and destination points (yellow arrow).

A pre-procedure 8-second C-arm CT scan (Siemens Healthineers, Erlangen, Germany) was performed on each vertebra. The reconstructed isotropic image voxel resolution was 0.46 mm^3. The resulting DICOM-format images were imported into 3D Slicer. After a volume rendering was computed, the fiducial markers were captured in the *Markups*

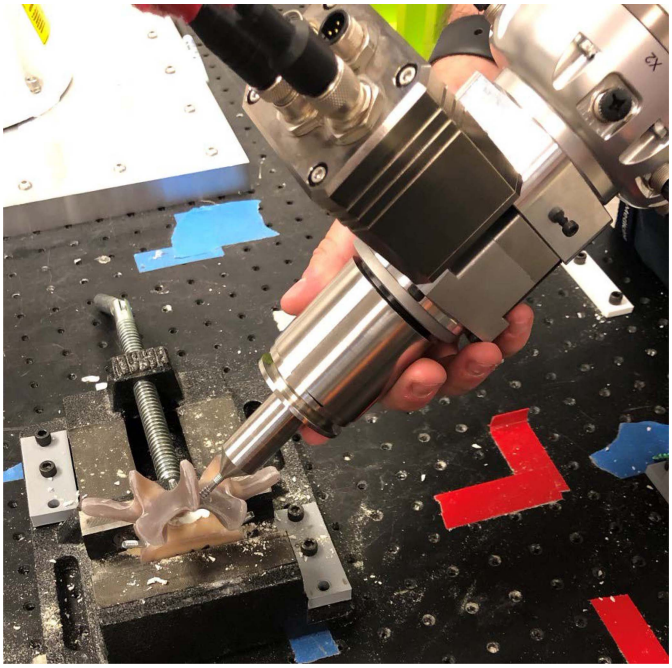

Fig. 8. Example of the process of hand-guiding the robot to a fiducial marker. At the request of the user, the robot program records the position of the robot end effector (which is located at a fiducial marker) to use in the image-to-robot coordinate system registration process.

Module using reformatted planar views and the volume rendering, as shown in Fig. 7. The same technique was then used to identify the entry and destination points of the desired screw locations (Fig. 7c). These data were then used to place two screws in each vertebra, as described above. The bones were then re-scanned in the same scanner, as shown in Fig. 10.

Screw placement accuracy was measured in 3D Slicer. The pre-procedure and post-procedure scans for a particular bone were imported, and their volumes were cropped so that a higher percentage of the image volume included the bone, markers, and screws. The *General Registration* module was then used to register the post-operative image to the pre-operative image. This module uses the image content rather than individual fiducial markers. The percentage of image volume samples used was set at 2%, and a rigid 6 degree-of-freedom registration was performed. The screw entry and destination points were then identified using the *Markups* module (Fig. 10), with the user blinded to the markers used in planning. The planned and measured screw locations were exported from 3D Slicer and then imported into a spreadsheet, were the errors were computed.

The entry point error was computed as the shortest distance between the measured entry point and the line connecting the planned entry and destination points. This is a more clinically relevant measurement than the distance between the two entry points and is consistent with the measurements made in the evaluation of other robotic spine surgery systems, e.g., in [26]. The destination point error was computed as the Euclidean distance between the planned and measured destination points. Whereas it was not the primary goal of the study, we also measured the execution time for both registration and screw placement.

TABLE II
SCREW PLACEMENT ACCURACY RESULTS

Screw Number	Entry Point Error (mm)	Destination Point Error (mm)	Planned Depth (mm)
1	0.43	1.42	38.5
2	0.21	0.89	36.4
3	0.30	0.93	39.1
4	0.34	2.24	38.1
5	0.59	2.11	34.4
6	0.46	1.83	40.2
7	0.68	1.16	35.6
8	0.74	1.53	41.2
9	0.60	1.20	39.8
10	0.50	1.56	30.5
Mean ± SD	**0.49 ± 0.17**	**1.49 ± 0.46**	**37.4 ± 3.2**

B. Results

The error measurement for each of the 10 screws is listed in Table II. The mean error was 0.49 ± 0.17 mm for the entry point and 1.49 ± 0.46 mm for the destination point. The average screw depth was 37.4 ± 3.2 mm. No breach of the pedicles by the screws was observed.

The average time required for registration of 5 fiducial markers was 1 minute, 48 seconds, and the average time required to drill a hole and place a screw was 10 minutes, 39 seconds.

V. DISCUSSION

It is useful to compare the results of this study to those of the current commercial spine surgery systems. While many studies report only clinical performance, such as the extent of pedicle breach as defined by the Gertzbein-Robbins scale [27], we found several studies where accuracy was reported in mm. Table III lists the results of the current study along with six studies of commercial robotic spine surgery systems, involving either cadavers or patients. The KUKA-based system performed well by comparison. However, performing this procedure on cadavers and patients is much more involved and will likely contribute additional error. For example, the drill and screw driver will need longer shafts to perform minimally invasive screw placement, which will increase the error. The registration will be applied to a larger working volume. Also, there will likely be additional error introduced by whatever mechanism will be integrated into the system to compensate for patient movement. Nevertheless, the results reported here represent a reasonable starting point.

It is also interesting to compare these results to our preliminary experiment, in which 30 desk screws were placed in a series of bovine femurs. In this previous experiment, the tools and tool exchanger were 3D printed in PLA, and the deck screws were free to angulate on the screw head, to follow the path created by the drill. The insertion and destination

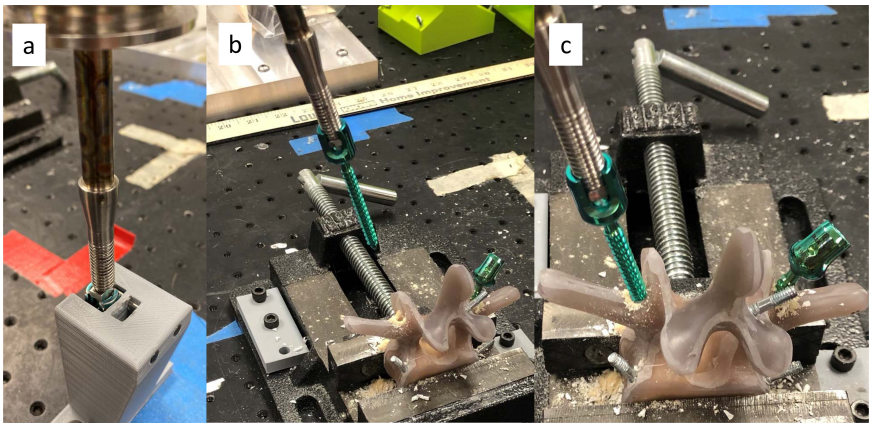

Fig. 9. Polyaxial screw pickup and placement process showing (a) driver picking up screw from rack, (b) robot angulating screw at a distance of 50 cm from entry point (to avoid facet contact), and (c) robot inserting screw.

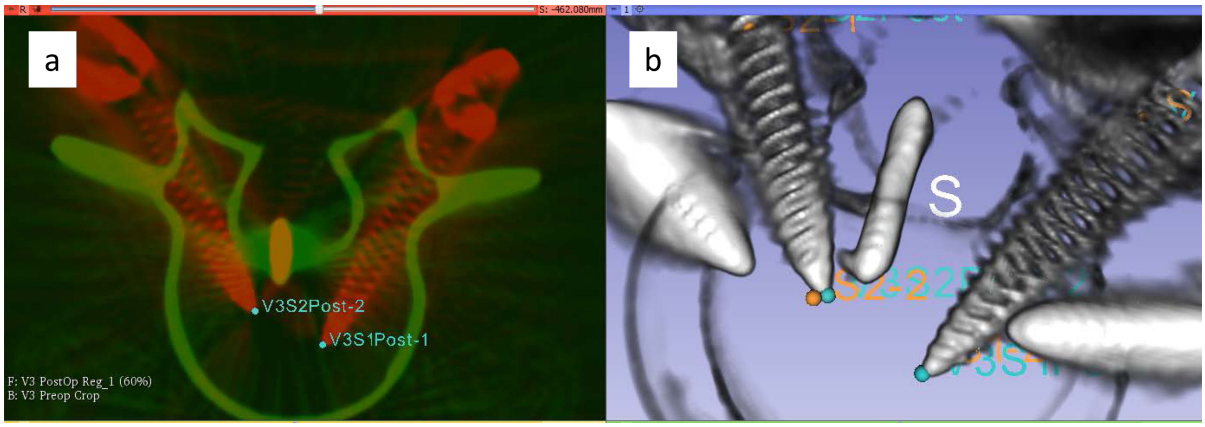

Fig. 10. (a) C-arm CT image of synthetic vertebra after robotic screw placement (red) registered with preoperative image (green) showing identification of destination points (cyan). (b) Volumetric rendering of postoperative C-arm CT image showing both the identified preoperative planned (orange) and postoperative measured (cyan) screw destination locations.

TABLE III
SCREW PLACEMENT ACCURACY COMPARISON TO COMMERCIAL ROBOT STUDIES

Authors	System	Subject	Number of Screws	Entry Point Error (mm)	Destination Point Error (mm)
Current study	KUKA-based	Synthetic Vertebrae	10	0.49 ± 0.17	1.49 ± 0.46
Togawa et al (28)	Mazor Renaissance	Cadaver	39	1.78 ± 0.58*	1.78 ± 0.58*
Lefranc and Peltier (11)	Rosa	Cadaver	38	2.05 ± 1.20	1.57 ± 1.01
Jiang et al (44)	ExcelsiusGPS	Patients	8	3.18 ± 1.29	2.11 ± 1.42
Godzik et al (12)	ExcelsiusGPS	Patients	116	5.20 ± 2.70	4.80 ± 2.40
Benech et al (43)	ExcelsiusGPS	Patients	292	2.30 ± 1.60	1.90 ± 1.60
Van Dijk et al (26)	Mazor Renaissance	Patients	178	2.00 ± 1.20	Not reported

* Devices were a combination of k-wires and pedicle screws. Placement error was measured as max[entry point error, destination point error].

accuracies for this experiment were 0.75 mm and 1.26 mm, respectively. The improvement in insertion accuracy (0.49 mm vs 0.75 mm, $p = 0.003$) over this preliminary test is likely due to switching from plastic to steel tools. The reduced volume range of the fiducial marker placement in the vertebrae could also have been a contributing factor, however most of these earlier femur experiments used 5 fiducials rather than 4, which anecdotally resulted in improved insertion accuracy. The decrease in destination accuracy (1.49 mm vs 1.26 mm, $p = 0.22$), while not statistically significant, may be due to a slight misalignment of the pedicle screw with respect to the screw driver shaft, combined with the properties of the vertebra test object. The synthetic vertebra has a thinner cortical bone section than the bovine femur, and a misaligned but rigidly held pedicle screw is able to move away from the planned path into softer cancellous bone during the rotation

and advancement of insertion. A custom designed combination of driver and screw should yield better destination accuracy.

With regard to execution time, we were extremely conservative in programming the motions of the robot, especially the tool exchange portions. Also, since we used a low speed drill, the drilling portion took over 3 minutes. With a higher speed drill and some further program optimization, we believe it will be straightforward to bring the procedure time per screw to less than 5 minutes.

The work presented here enables application of machine learning algorithms to spine screw insertion. For example, as the robot inserts the screw, it can measure the force and torque being applied to the screw and make adjustments in real time. The robot could also receive imaging information in real time and incorporate that into its insertion algorithm. Surgeons do this now, qualitatively, but perhaps not to the extent that would be possible with a computer algorithm, monitored by the surgeon. The goal of the current study was to develop a more precise and standardized process by which the spine can be instrumented. One could envision a very tightly integrated robot and imaging system, where 3D images are captured in real-time to guide the procedure. Parameters such as preoperatively (or even intraoperatively) measured bone density along with desired degrees of correction in a spinal deformity case, patient age, and length of instrumentation construct could be inserted into the integrated robot/computer system. The system then could determine the ideal screw diameter (which is correlated most closely to pullout strength), screw length, and thread pitch to allow for the best possible chances of a successful and lasting instrumentation and ultimately, fusion [29], [30], [31]. In such a complex system, there would be an ideal screw trajectory for the robot. In this scenario, given the precise forces required to place a screw without stripping the bone, the task would need to be left to the accuracy of a robot instead of a human hand through a guide tube.

There are several potential benefits to automating spine screw insertion, and other image-guided surgical tasks. Spine screw placement automation would enable procedures to be performed remotely, with other medical personnel assisting onsite. This capability would be beneficial to patients in remote geographic areas (including outer space), patients in battle zones, and even patients in need of surgery during a pandemic. Remote capability would enable community surgeons to collaborate with world-class surgeons to offer technically complex procedures to the local population. Since it has been shown that surgical outcomes often are correlated directly with case volume of the particular surgery in a given institution, it makes sense to have rarely done procedures performed remotely at the hands of a high-volume surgeon given a particular technique or surgery [32]. This becomes especially true as the Centers for Medicare and Medicaid Services is increasingly focused on patient outcomes, which affect both payments and penalties [33].

Screw placement automation also relieves the surgeon of many of the physical constraints of the procedure. This includes both fatigue for long procedures and also the manual dexterity required to perform spine surgery (some of which is alleviated by current systems). The physical challenges involved in performing these procedures cause long-term health effects for spine surgeons [34], [35]. In one study, 60% of spine surgeons reported neck-related musculoskeletal disorders (MSD), and 49% reported shoulder-related MSD's [34]. Spine surgeons are also 10 times more likely to require cervical disk surgery than the general population [34]. While we found no breakdown of the most harmful repetitive motions in fusion surgery (what Abshire *et al.* termed "long duration, repetitive, forceful tasks [34]), the neurosurgeon author of this work (Birinyi) estimates that up to 90% of these motions are related to the drilling and screw placement portions of the procedure, and that drilling and screw placement constitute 25%-50% of the overall procedure time.

Not only does the current system eliminate the requirement to manually apply force and torque during placement, but it also eliminates many of the challenging and harmful body positions surgeons must assume during the procedure. In contrast, the physical challenges of drilling and screw placement are still present in current guide-tube-based spine surgery robots. The reduction in the physical requirements of the procedure also enables the surgeon to act as the manager rather than the mechanic, and to spend more time planning and evaluating, rather than executing, the procedure. Finally, aging surgeons can have difficulty maintaining the stamina required for long-segment spinal fusion/instrumentation procedures and can develop a decline in their technical abilities [31]. With ongoing physician shortages and cognitively-competent but aging surgeons, a means to provide surgeons with the benefits of their youth is welcome in the surgical fields [32].

Overall, while automation of the screw placement process is not necessary to perform spinal surgery, we predict that automation, once perfected, will become the mainstay in spinal surgery just as automation has become the mainstay in the automotive manufacturing industry despite the obvious ability to build a car by hand. Accuracy and precision along with objective measurement feedback from a robot like the one we describe have the potential always to be superior in a machine compared to these features in a human. Finally, other parts of the procedure, such as resection [36] and suturing [37] are also being automated.

The system overall will require further development prior to human use. Whereas the robot used its own internal localization capability for navigation, the system is currently unable to track patient movement, a critical feature for a clinical system. While a navigation system could be integrated, a fixed x-ray system could also be used to detect movement and correct the registration [38]. It would also be straightforward to obviate the need to implant and touch fiducial markers by having the robot hold a radiopaque fiducial marker pattern such that it was included in an intra-operative image, as is done with the commercial robotic spine surgery systems.

There are many features inherent to the robot that can be exploited to enhance the functionality of the system. The robot can be programmed to detect collisions with humans. The robot can also measure both force and torque on each axis. Since axis 7 (the most distal axis) is aligned with the end effector axis, it can be used to measure the force and torque applied to the drill or screw driver throughout the procedure, which can

be used to make decisions based on these values, and which could be incorporated into machine learning algorithms.

The current system has a rudimentary user interface, with only the start and end point of the screw being specified, and no feedback provided to the user during screw insertion. Using the internal localization capability of the robot, it would be possible to provide the real-time screw location to the user in 3D Slicer, during the screw insertion process. CAD models of various screws could be used for planning, as with the current commercial systems.

The KUKA LBR has been used as the basis for several robotic surgery systems. Dwyer *et al.* developed a programmable robotic endoscope holder, based on the KUKA LBR, for an imaging application in fetoscopy [39]. Virga *et al.* integrated a KUKA LBR into a system designed to perform automated ultrasound scans in patients, for the purpose of diagnosis abdominal aortic aneurysms [40]. Augello *et al.* developed an image-guided, robotic laser osteotomy system, based on the KUKA LBR [41]. Kojev *et al.* developed a KUKA LBR dual-robot system for ultrasound-guided needle placement [42]. One could envision a scenario where a hospital would own one robot that was used for multiple applications, thereby reducing the overall equipment cost. The system described in this work could be developed for multiple spine-related applications, including image-guided laminectomy.

VI. Conclusion

To our knowledge, this is the first system that has demonstrated the potential to automate polyaxial spine screw placement completely as a *supervisory controlled autonomous robot*. Furthermore, the accuracy compares favorably to the current commercially available systems that operate as *shared control robots*, although the test conditions were more favorable than for those evaluations. Further development and testing are underway.

Acknowledgment

The authors would like to thank Philippe Mercier and Richard Bucholz from the Department of Neurosurgery at Saint Louis University School of Medicine for their feedback and advice. They would also like to thank Tom Uxa and Shane Hammond at J&S Tool for their custom drill bit machining. They would like to thank Michael Andrus for illustrating Fig. 1.

References

[1] S. Sajeev and G. Chandra, *Global Surgical Robotics—Market Opportunities and Forecasts 2017–2024*, Allied Market Res., Portland, OR, USA, 2018.

[2] *Surgical Robots Market Size, Share & Trends*, Grand View Res., San Francisco, CA, USA, 2019.

[3] *Surgical Robots Market by Component*, Markets Markets, Pune, India, 2018.

[4] M. T. Modic and J. S. Ross, "Lumbar degenerative disk disease," *Radiology*, vol. 245, no. 1, pp. 43–61, 2007.

[5] F. M. Phillips, P. J. Slosar, J. A. Youseff, G. Andersson, and F. Papatheofanis, "Lumbar spine fusion for chronic low back pain due to degenerative disc disease: A systematic review," *SPINE*, vol. 38, no. 7, pp. E409–E422, 2013.

[6] Y. Barzilay, M. Liebergall, A. Fridlander, and N. Knoller, "Miniature robotic guidance for spine surgery—Introduction of a novel system and analysis of challenges encountered during the clinical development phase at two spine centers," *Int. J. Med. Robot. Comput. Assist. Surg.*, vol. 2, no. 2, pp. 146–153, 2006.

[7] J. Merlet, *Parallel Robots*. Dordrecht, The Netherlands: Springer, 2006.

[8] *Mazor X Stealth Edition*, Medtronic, Minneapolis, MN, USA, Feb. 2019. Accessed: Dec. 19, 2019. [Online]. Available: https://www.medtronic.com/us-en/healthcare-professionals/products/neurological/spine-robotics/mazorx.html

[9] K. R. Smith, K. J. Frank, and R. D. Bucholz, "The *Neurostation*^{TM}—A highly accurate, minimally invasive solution to frameless stereotactic neurosurgery," *Comput. Med. Imag. Graph.*, vol. 18, no. 4, pp. 247–256, 1994.

[10] G. D. Ioannis *et al.*, "Accuracy of pedicle screw placement: A systematic review, of prospective in vivo studies comparing free hand, fluoroscopy guidance and navigation techniques," *Eur. Spine J.*, vol. 21, pp. 247–255, Feb. 2012.

[11] M. LeFranc and J. Peltier, "Accuracy of thoracolumbar transpedicular and vertebral body percutaneous screw placement: Coupling the Rosa® Spine robot with intraoperative flat-panel CT guidance—A cadaver study," *J. Robot. Surg.*, vol. 9, pp. 331–338, Dec. 2015.

[12] J. Godzik *et al.*, "A quantitative assessment of the accuracy and reliability of robotically guided percutaneous pedicle screw placement: Technique and application accuracy," *Oper. Neurosurg.*, vol. 17, no. 4, pp. 389–395, 2019.

[13] *Mazor Robotics—FAQ for Surgeons*, Medtronic, Minneapolis, MN, USA, May 2018. Accessed: Dec. 19, 2019. [Online]. Available: https://www.mazorrobotics.com/en/resources/for-surgeons/faq-for-surgeons

[14] J. D. Stull, J. J. Mangan, A. R. Vaccaro, and G. D. Schroeder, "Robotic guidance in minimally invasive spine surgery: A review of recent literature and commentary on a developing technology," *Current Rev. Musculoskeletal Med.*, vol. 12, pp. 245–251, Jun. 2019.

[15] A. Ghasem, A. Sharma, D. N. Greif, M. Alam, and M. Al Maaieh, "The arrival of robotics in spine surgery," *Spine*, vol. 43, no. 23, pp. 1670–1677, 2018.

[16] B. N. Staub and S. S. Sadrameli, "The use of robotics in minimally invasive spine surgery," *J. Spine Surg.*, vol. 5, pp. S31–S40, Jun. 2019.

[17] B. Fiani, S. A. Quadri, M. Farooqui, A. Cathel, and B. Berman, "Impact of robot-assisted spine surgery on health care quality and neurosurgical economics: A systemic review," *Neurosurg. Rev.*, vol. 43, pp. 17–25, Feb. 2020.

[18] J. R. Joseph, B. W. Smith, X. Liu, and P. Park, "Current applications of robotics in spine surgery: A systematic review of the literature," *Neurosurg. Focus*, vol. 42, p. E2, May 2017.

[19] T. Ortmaier, H. Weiss, S. Dobele, and U. Schreiber, "Experiments on robot-assisted navigated drilling and milling of bones for pedicle screw placement," *Int. J. Med. Robot. Comput. Assist. Surgery*, vol. 2, pp. 350–363, Dec. 2006.

[20] S. Kim, J. Chung, B.-J. Yi, and Y. S. Kim, "An assistive image-guided surgical robot system using O-arm fluoroscopy for pedicle screw insertion: Preliminary and cadaveric study," *Neurosurgery*, vol. 67, no. 6, pp. 1757–1767, 2010.

[21] W. Tian *et al.*, "A robot-assisted surgical system using a force-image control method for pedicle screw insertion," *PLoS ONE*, vol. 9, no. 1, 2014, Art. no. e86346.

[22] R. H. Taylor and D. Stoianovici, "Medical robotics in computer-integrated surgery," *IEEE Trans. Robot. Autom.*, vol. 19, no. 5, pp. 765–781, Oct. 2003.

[23] N. Nathoo, M. C. Cavusoglu, M. A. Vogelbaum, and G. H. Barnett, "In touch with robotics: Neurosurgery for the future," *Neurosurgery*, vol. 56, no. 3, pp. 421–433, 2005.

[24] J. Tokuda *et al.*, "OpenIGTLink: An open network protocol for image-guided therapy environment," *Int. J. Med. Robot. Comput. Assist. Surg.*, vol. 5, pp. 423–434, Dec. 2009.

[25] K. S. Arun, T. S. Huang, and S. D. Blostein, "Least-squares fitting of two 3-D point sets," *IEEE Trans. Pattern Anal. Mach. Intell.*, vol. PAMI-9, no. 5, pp. 698–700, Sep. 1987.

[26] J. D. van Dijk, R. P. van den Ende, S. Stramigioli, M. Kochling, and N. Hoss, "Clinical pedicle screw accuracy and deviation from planning in robot-guided spine surgery: Robot-guided pedicle screw accuracy," *Spine*, vol. 40, no. 17, pp. E986–E991, 2015.

[27] S. D. Gertzbein and S. E. Robbins, "Accuracy of pedicle screw placement in vivo," *Spine*, vol. 15, no. 1, pp. 11–14, 1990.

[28] D. Togawa *et al.*, "Bone-mounted miniature robotic guidance for pedicle screw and translaminar facet screw placement: Part 2–Evaluation of system accuracy," *Neurosurgery*, vol. 60, pp. ONS129–ONS139, Feb. 2007.
[29] J. Morche, T. Mathes, and D. Pieper, "Relationship between surgeon volume and outcomes: A systematic review of systematic reviews," *Syst. Rev.*, vol. 5, no. 204, p. 204, 2016.
[30] *Value-Based Programs*, U.S. Centers Medicare Medicaid Serv., Baltimore, MD, USA, Jan. 2020. Accessed: Aug. 27, 2020. [Online]. Available: https://www.cms.gov/Medicare/Quality-Initiatives-Patient-Assessment-Instruments/Value-Based-Programs/Value-Based-Programs
[31] *Statement on the Aging Surgeon*, Amer. Coll. Surg., Chicago, IL, USA, Jan. 2016. Accessed: Aug. 27, 2020. [Online]. Available: https://www.facs.org/about-acs/statements/80-aging-surgeon
[32] C. W. Van Way, III, "Is there a surgeon shortage?" *Missouri Med.*, vol. 107, no. 5, pp. 309–312, 2010.
[33] T. O. McKinley, R. F. McLain, S. A. Yerby, N. A. Sharkey, N. Klijin, and T. S. Smith, "Characteristics of pedicle screw loading. Effect of surgical technique on intravertebral and intrapedicular bending moments," *Spine*, vol. 24, no. 1, pp. 18–24, 1999.
[34] B. B. Abshire, R. F. McLain, A. Valdevit, and H. E. Kambic, "Characteristics of pullout failure in conical and cylindrical pedicle screws after full insertion and back-out," *Spine J.*, vol. 1, no. 6, pp. 408–414, 2001.
[35] M. H. Krenn and W. P. Piotrowski, "Influence of thread design on pedicle screw fixation. Laboratory investigation," *J. Neurosurg. Spine SPI*, vol. 9, no. 1, pp. 90–95, 2008.
[36] P. Shi *et al.*, "A soft tissue scalpel cutting robotic system with sucker fixation," in *Proc. IEEE 14th Int. Conf. Control Autom. (ICCA)*, Anchorage, AK, USA, 2018, pp. 1162–1167.
[37] A. Krieger, J. Opfermann, and P. C. Kim, "Development and feasibility of a robotic laparoscopic clipping tool for wound closure and anastomosis," *J. Med. Devices*, vol. 12, no. 1, p. 6, 2018.
[38] T. Yi, V. Ramchandran, J. Siewerdsen, and A. Uneri, "Robotic drill guide positioning using known-component 3D–2D image registration," *J. Med. Imag.*, vol. 5, no. 2, 2018, Art. no. 021212.
[39] G. Dwyer, R. J. Colchester, E. J. Alles, E. Maneas, and S. Ourselin, "Robotic control of a multi-modal rigid endoscope combining optical imaging with all-optical ultrasound," in *Proc. Int. Conf. Robot. Autom.*, Montreal, QC, Canada, 2019, pp. 3882–3888.
[40] S. Vigra, O. Zettnig, M. Esposito, K. Pfister, and B. Frisch, "Automatic force-compliant robotic ultrasound screening of abdominal aortic aneurysms," in *Proc. IEEE/RSJ Int. Conf. Intell. Robots Syst.*, Daejeon, South Korea, 2016, pp. 508–513.
[41] M. Augello, C. Baetscher, M. Segesser, H.-F. Zeilhofer, and P. Cattin, "Performing partial mandibular resection, fibula free flap reconstruction and midfacial osteotomies with a cold ablation and robot-guided Er:YAG laser osteotome (CARLO®)—A study on applicability and effectiveness in human cadavers," *J. Cranio Maxillo Facial Surg.*, vol. 46, pp. 1850–1855, Oct. 2018.
[42] R. Kojcev *et al.*, "Dual-robot ultrasound-guided needle placement: Closing the planning-imaging-action loop," *Int. J. Comput. Assist. Radiol. Surg.*, vol. 11, pp. 1173–1181, Apr. 2016.
[43] C. A. Benech, R. Perez, F. Benech, S. L. Greeley, N. Crawford, and C. Ledonio, "Navigated robotic assistance results in improved screw accuracy and positive clinical outcomes: An evaluation of the first 54 cases," *J. Robot. Surg.*, vol. 14, pp. 431–437, 2020. [Online]. Available: https://doi.org/10.1007/s11701-019-01007-z
[44] B. Jiang *et al.*, "Pedicle screw accuracy assessment in ExcelsiusGPS® robotic spine surgery: Evaluation of deviation from pre-planned trajectory," *Chin. Neurosurg. J.*, vol. 4, p. 23, 2018.

Alexander D. Smith was born in West Linn, OR, USA, in 1997. He received the B.S. degree with a double major in biomedical engineering and computer science from Saint Louis University in 2019. He is currently pursuing the M.D./Ph.D. degrees with the Carle-Illinois College of Medicine.

From 2015 to 2019, he worked as a Research Intern with Andrew Hall's Laboratory, Saint Louis University. From 2019 to 2020, he was a Research Assistant with the Carnegie Center for Surgical Innovation, Johns Hopkins Hospital. He has authored five articles and two inventions. His research interests include cognitive neuroscience, computational medicine, medical robotics, and surgical instrumentation design and innovation.

Jacob Chapin was born in Saint Louis, MO, USA, in 1996. He received the B.S. degree in biomedical engineering from Saint Louis University in 2018, and the M.S. degree in engineering with an emphasis in biomedical engineering in 2019.

From 2016 to 2019, he worked in Andrew Hall's laboratory at Saint Louis University focusing on automated screw placement. His research interests include medical robotics, 3-D printing for medical imaging applications, and surgical instrumentation design and innovation.

Paul V. Birinyi was born in Dallas, TX, USA. He received the B.A. and M.S. degrees in neuroscience (cellular and molecular concentration) from Johns Hopkins University, Baltimore, MD, USA, in 2006, and the M.D. degree from UT Southwestern Medical School, Dallas, in 2010. He is currently in a Private Neurosurgical Practice in Alexandria, LA, USA, specializing in minimally invasive spinal procedures and functional neurosurgery.

He completed his neurological surgery residency at Saint Louis University, St. Louis, MO, USA, in 2017. He achieved the neurosurgical specialization by completing a Neurosurgical Spine Fellowship under the direction of Dr. K. Foley with the Semmes-Murphey Clinic/University of Tennessee Health Science Center, Memphis, TN, USA, in 2018. He has been involved extensively with medical students and resident education through his authorship of a neurosurgical textbook and years of teaching anatomy. His research interests have included, restless legs syndrome and alcohol and drug addiction, a passion he pursued performing research with the National Institutes on Drug Abuse, Baltimore, MD, USA. His current interests include medical device development and creating and integrating robotics and computer-assisted navigation technologies.

Prathamesh V. Bhagvath was born in Mumbai, India, in 1991. He received the B.S. degree in biomedical engineering from the University of Mumbai in 2013, and the M.S. degree in biomedical engineering from the University of Bridgeport in 2016. He is currently pursuing the Ph.D. degree in engineering with Saint Louis University with an emphasis in surgical robotics.

From 2016 to 2019, he worked as a Medical Device Validation Engineer with Baxter and Biomerieux. As a Research Assistant in Andrew Hall's laboratory, his work is focused on improving automation in spine surgery and developing machine learning techniques in robotic surgery. His research interests include image-guided surgical robotics, machine learning in surgical applications, 3-D printing, and interventional medical device design.

Andrew F. Hall (Member, IEEE) was born in Granite City, IL, USA, in 1959. He received the B.S. degree in electrical engineering from Southern Illinois University, Carbondale, in 1982, and the M.S. degree in electrical engineering and the D.Sc. degree in biomedical engineering from Washington University in St. Louis in 1989 and 1997, respectively. He has been an Associate Professor of Biomedical Engineering with the Parks College of Engineering, Aviation and Technology, Saint Louis University in St. Louis, MO, USA, since 2014.

From 1997 to 2005, he worked in interventional robotics research and development for medical device startup Stereotaxis, Inc. From 2005 to 2014, he worked as a Research Collaborations Director with the Angiography Division of Siemens Medical Solutions USA, Inc. His research interests include imaging in interventional radiology, 3-D printing for medical imaging applications, medical robotics, and interventional medical devices.